ISSN (Print) 1226-1750
ISSN (Online) 2233-6656
Journal of Magnetics 23(2), 196-200 (2018) https://doi.org/10.4283/JMAG.2018.23.2.196

Ferrimagnetic Domain Wall Motion Induced by Damping-like Spin-orbit Torque

Se-Hyeok Oh[1] and Kyung-Jin Lee[1,2,3]*

[1]*Department of Nano-Semiconductor and Engineering, Korea University, Seoul 02841, Korea*
[2]*Department of Materials Science and Engineering, Korea University, Seoul 02841, Korea*
[3]*KU-KIST Graduate School of Converging Science and Technology, Korea University, Seoul 02841, Korea*

(Received 8 May 2018, Received in final form 15 June 2018, Accepted 19 June 2018)

We theoretically and numerically investigate ferrimagnetic domain wall motion driven by damping-like spin-orbit torque. We find that the damping-like spin-orbit torque combined with the interfacial Dzyaloshinskii-Moriya interaction efficiently drives the ferrimagnetic domain wall especially at the angular momentum compensation point. We obtain the analytic expression of the domain wall velocity with respect to the current density and the net spin density, which is in agreement with numerical simulation. The analytic expression is applicable to arbitrary compensation conditions, ranging from the ferromagnetic limit to the antiferromagnetic limit, and is thus useful to design and interpret ferrimagnetic domain wall experiments at various temperatures or compositions.

Keywords : Ferrimagnetic domain wall, Spin-orbit torque, Dzyaloshinskii-Moriya interaction, Angular momentum compensation

1. Introduction

Magnetic domain walls can be used as information carriers and enable the realization of magnetic logic and storage devices [1, 2]. The domain wall motion is induced by magnetic fields [3, 4], propagating spin waves [5-10], spin-transfer torques [11-13], and spin-orbit torques [14-16]. Among them, the electrical means (i.e., spin-transfer torques and spin-orbit torques) is adequate for practical applications because it moves multiple domain walls in the same direction at a relatively high speed. Two essential requirements for high-density and energy-efficient domain wall devices are the small-sized domain wall and its fast motion [17]. The small-size requirement favors to use perpendicular domain walls [18, 19]. On the other hands, the high-speed requirement leads to a recent interest in the spin-orbit torque originating from the spin-orbit interaction in magnetic/non-magnetic heterostructures [20-28]. In particular, recent theoretical and experimental studies emphasize the importance of three-dimensional spin transport to understand spin-orbit torques in heterostructures [29-36].

The spin-orbit torque combined with the interfacial Dzyaloshinskii-Moriya interaction (DMI) drives magnetic domain walls efficiently [14-16]. In case of ferromagnetic domain walls, the spin-orbit torque tilts the domain wall angle so that the ferromagnetic domain wall velocity saturates with increasing the current density [14]. This velocity saturation can be avoided by employing antiferromagnetic domain walls, as the domain wall angle is completely decoupled from the domain wall position and thus does not tilt [37]. Despite the outstanding advantage of the antiferromagnetic domain walls, the manipulation and the detection of antiferromagnetic spin textures in true antiferromagnets are challenging because of zero net magnetic moment. A way to partially overcome this challenge is to use synthetic antiferromagnets [38, 39] where the net magnetic moment varies with the thicknesses of two ferromagnets coupled antiferromagnetically. However, perfect antiferromagnetic textures in synthetic antiferromagnets still suffer from zero net moment.

In our previous work [40], we focused mainly on the field-driven domain wall motion in rare-earth (RE)-transition metal (TM) ferrimagnets and addressed the damping-like-torque-driven ferrimagnetic domain wall motion only at the angular momentum compensation point. When driven by a damping-like torque, the ferrimagnetic domain wall velocity at the angular momentum compen-

*Corresponding author: Tel: +82-2-3290-3289
Fax: +82-2-928-3584, e-mail: kj_lee@korea.ac.kr

sation point is found to be qualitatively identical to the antiferromagnetic domain wall velocity [37, 40]. In this work, we report a theoretical study on detailed ferrimagnetic domain wall dynamics driven by damping-like torque for arbitrary compensation conditions. The field-like torque directly competes with the antiferromagnetic exchange torque that is usually much stronger than the field-like torque. As a result, we neglect the field-like torque in our study. We believe that a theoretical prediction for arbitrary conditions is important to design domain wall experiments and to interpret experimental results for the fundamental understanding of ferrimagnetic domain wall dynamics and the improved performance of ferrimagnetic domain wall devices.

We first derive the equations of motion for ferrimagnetic domain wall with the collective coordinate approach [40-44]. To start with the continuum approximation, we define the staggered vector $\mathbf{n} = (\mathbf{m}_1 - \mathbf{m}_2)/2$ and the magnetization vector $\mathbf{m} = \mathbf{m}_1 + \mathbf{m}_2$, where $\mathbf{m}_1$ and $\mathbf{m}_2$ are the unit vectors of magnetic moments at two sublattices (RE and TM). The sublattice i has the magnetic moment M_i and the magnitude of the spin density $s_i = M_i/\gamma_i$, where $\gamma_i = g_i\mu_B/\hbar$ is the gyromagnetic ratio, μ_B is the Bohr magneton, and g_i is the Landé-g factor. We define $s = (s_1 + s_2)/2$, and the net spin density $\delta_s = s_1 - s_2$.

The general Lagrangian density $\mathcal{L}$ for ferrimagnets is described by [40, 41, 45]

$$\mathcal{L} = \rho\dot{\mathbf{n}}/2 - \delta_s \mathbf{a}[\mathbf{n}]\cdot\mathbf{n} - \mathcal{U}, \tag{1}$$

where ρ parametrizes the inertia of the dynamics, $\mathbf{a}[\mathbf{n}]$ is the vector potential generated by a magnetic monopole of unit charge satisfying $\nabla_{\mathbf{n}} \times \mathbf{a} = \mathbf{n}$, and $\mathcal{U}$ is the potential energy density. The first term on the right-hand side is the spin Berry phase associated with the staggered spin density, and the second term is the Berry phase associated with δ_s. We consider the potential-energy density including the interfacial DMI as

$$\mathcal{U} = \frac{a}{2}|\mathbf{m}|^2 + \frac{A}{2}(\nabla\mathbf{n})^2 - \frac{K}{2}(\mathbf{n}\cdot\hat{\mathbf{z}})^2 + \frac{\kappa}{2}(\mathbf{n}\cdot\hat{\mathbf{x}})^2 + \frac{D}{2}\hat{\mathbf{y}}\cdot(\mathbf{n}\times\partial_x\mathbf{n}), \tag{2}$$

where a and A are the homogeneous and inhomogeneous exchange energy constants, respectively, K is the easy-axis anisotropy energy constant, κ is the hard-axis anisotropy constant, and D is the interfacial DMI energy constant. We introduce the Rayleigh dissipation function for the energy dissipation as $\mathcal{R} = \alpha s\dot{\mathbf{n}}^2$, where α is the Gilbert damping constant.

From the Lagrangian density and Rayleigh dissipation function, we obtain the equations of motion for **n** and **m**. Including the damping-like torque, two equations of motion for **n** and **m** are given as

$$\frac{\partial\mathbf{n}}{\partial t} = -\frac{1}{s}\mathbf{f}_m\times\mathbf{n} + \mathbf{T}_n, \tag{3}$$

$$\frac{\partial\mathbf{m}}{\partial t} = -\left(\frac{1}{s}\mathbf{f}_n - 2\alpha\frac{\partial\mathbf{n}}{\partial t}\right)\times\mathbf{n} - \frac{\delta_s}{s}\frac{\partial\mathbf{n}}{\partial t} + \mathbf{T}_m, \tag{4}$$

where $\mathbf{T}_n = (\delta_s\tilde{B}_D/2)\mathbf{n}\times(\mathbf{n}\times\hat{\mathbf{y}})$, $\mathbf{T}_m = -2s\tilde{B}_D\mathbf{n}\times(\mathbf{n}\times\hat{\mathbf{y}})$, $\mathbf{f}_{n(\mathrm{m})} = -\delta\mathcal{U}/\delta\mathbf{n}(\mathbf{m})$, $\tilde{B}_D = \hbar\theta_{SH}J/2et_z s_1 s_2$, θ_{SH} is the effective spin Hall angle, J is the current density, e is the charge, and t_z is the thickness of ferrimagnetic layer. Here $\mathbf{T}_n$ and $\mathbf{T}_m$ are obtained from the damping-like torque term for the discrete spin model, $(\partial\mathbf{S}_i/\partial t) = -\gamma_i B_{D,i}\mathbf{S}_i\times(\mathbf{S}_i\times\hat{\mathbf{y}})$, where $B_{D,i} = \hbar\theta_{SH}J/2eM_i t_z$ is the effective field for the damping-like torque.

We introduce the collective coordinates for the domain wall position X and the domain wall angle ϕ, with the ansatz for the wall profile [46]: $\mathbf{n}(x,\mathrm{t}) = (\sin\theta\cos\phi, \sin\theta\sin\phi, \cos\theta)$, where $\theta = 2\tan^{-1}\{\exp[(x-X)/\lambda]\}$ and λ is the domain wall width. By proceeding with the same manner as in Ref. [40], we obtain two equations of motion:

$$M\ddot{X} - G\dot{\phi} + M\left(\frac{1}{\tau} - \frac{\pi}{8}\delta_s\tilde{B}_D\sin\phi\right)\dot{X} = -2s^2\pi\tilde{B}_D\mathcal{A}\cos\phi, \tag{5}$$

$$I\ddot{\phi} + G\dot{X} + I\left(\frac{1}{\tau} - \frac{\pi}{8}\delta_s\tilde{B}_D\sin\phi\right)\dot{\phi} = -\tilde{\kappa}\sin\phi\cos\phi + \tilde{D}\sin\phi. \tag{6}$$

Here $M = 2\rho\mathcal{A}/\lambda$ is the mass, $I = 2\rho\lambda\mathcal{A}$ is the moment of inertia, $G = 2\delta_s\mathcal{A}$ is the gyrotropic coefficient, $\tau = \rho/2\alpha s$ is the relaxation time, $\tilde{\kappa} = 2\kappa\lambda\mathcal{A}$, $\tilde{D} = \pi D\mathcal{A}/2$, and $\mathcal{A}$ is the cross-sectional area of the domain wall. One finds from Eqs. (5) and (6) that the domain wall position X and angle ϕ are coupled through the gyrotropic coefficient G, which is proportional to δ_s. When δ_s is nonzero, the translational motion of domain wall is inevitably combined with the precession motion of domain wall. In other words, the angular momentum supplied by the damping-like torque is used not only to move a domain wall but also to rotate a domain wall angle. On the other hands, when δ_s is zero, the angular momentum gain is used only for the domain wall motion because ϕ does not change with time. From Eqs. (5) and (6), we obtain the steady-state solution for domain wall velocity v_{DW}, which is the central result in this paper, as

$$v_{DW} = -\frac{8s^2\pi\lambda\tilde{B}_D\cos\phi_{st}}{16\alpha s - \rho\pi\delta_s\tilde{B}_D\sin\phi_{st}}, \tag{7}$$

which ϕ_{st} is the steady-state solution of ϕ. We note that Eq. (7) is general and applicable not only to ferrimagnetic domain walls but also to ferromagnetic or antiferromagnetic domain walls. The ratio of the net spin density δ_s to s describes the degree of *ferromagneticity*. When

$\delta_s / 2s \to \pm 1$, it approaches the ferromagnetic limit. On the other hands, $\delta_s / 2s \to 0$ indicates the antiferromagnetic limit. One can conceptually understand the features of ferrimagnetic domain wall dynamics driven by damping-like torque by analyzing Eqs. (5), (6), and (7). In the strong DMI limit, the domain wall angle in the absence of the current is 0 or π (thus, $\cos\phi_{st} = \pm 1$). In the ferromagnetic limit, the domain wall angle increases with the current density J so that $|\cos\phi_{st}|$ decreases with increasing J. Combined with the linear increase of $\tilde{B}_D$ in Eq. (7), the domain wall velocity saturates as the current increases [14]. This correlation is mediated by the gyrotropic coefficient G that couples $\dot{X}$ with $\dot{\phi}$ in Eqs. (5) and (6). In the antiferromagnetic limit, however, this coupling is absent because $G = 0$. As a result, the domain wall velocity can increase linearly with the current, which is analogous with the case of true antiferromagnetic domain walls [37].

To verify Eq. (7), we conduct numerical calculations with the atomistic Landau-Lifshitz Gilbert equation including the damping-like torque:

$$\frac{\partial \mathbf{S}_i}{\partial t} = -\gamma_i \mathbf{S}_i \times \mathbf{B}_{eff,i} + \alpha \mathbf{S}_i \times \frac{\partial \mathbf{S}_i}{\partial t} - \gamma_i B_{D,i} \mathbf{S}_i \times (\mathbf{S}_i \times \hat{\mathbf{y}}), \quad (8)$$

where $\mathbf{B}_{eff,i} = -(1/\mu_i)\partial\mathcal{H}/\partial\mathbf{S}_i$ is the effective field, μ_i is the magnetic moment per atom, and $\mathbf{S}_i$ is the normalized spin moment vector at lattice site i. The one-dimensional discrete Hamiltonian $\mathcal{H}$ is given by

$$\mathcal{H} = A_{sim} \sum_i \mathbf{S}_i \cdot \mathbf{S}_{i+1} - K_{sim} \sum_i (\mathbf{S}_i \cdot \hat{\mathbf{z}})^2 + \kappa_{sim} \sum_i (\mathbf{S}_i \cdot \hat{\mathbf{x}})^2 + D_{sim} \sum_i \hat{\mathbf{y}} \cdot (\mathbf{S}_i \times \mathbf{S}_{i+1}), \quad (9)$$

where A_{sim} is the exchange constant, K_{sim} is the easy-axis anisotropy, κ_{sim} is the hard-axis anisotropy, and D_{sim} is the DMI constant. The relations for the material parameters between Eqs. (2) and (9) are $A = 4A_{sim}/d$, $a = 4A_{sim}/d^2$, $K = 2K_{sim}/d^3$, $\kappa = 2\kappa_{sim}/d^3$, and $D = 8D_{sim}/d^2$. We use the following parameters for numerical simulations: $A_{sim} =$ 7.5 meV, $K_{sim} = 0.08$ meV, $\kappa_{sim} = 0.08$ μeV, $D_{sim} = 0.05$ meV, $\alpha = 0.02$, $\theta_{SH} = 0.1$, and $g_{TM(RE)} = 2.2(2.0)$ [47]. The thickness of ferrimagnetic layer and lattice parameter $t_z = d = 0.4$ nm. The magnetic moments $M_{TM,RE}$ used in the numerical calculations are shown in Table 1.

Figure 1 shows the velocity of ferrimagnetic domain wall as a function of δ_s at various current densities. Symbols obtained from numerical calculation are in good agreement with the analytical solution, Eq. (7). In low current regime, the velocity is almost constant, whereas in high current regime ($J \geq 3\times10^{11}$ A/m^2) it shows the maximum at the angular momentum compensation point (i.e., $\delta_s = 0$). The velocity gradually decreases with increasing $|\delta_s|$. Figure 2 shows the domain wall angle ϕ as a function of δ_s at various current densities. The DMI

Table 1. The magnetic moments M_{TM} for the transition metal element and M_{RE} for the rare-earth element, used in the numerical calculation. Index represents the parameter set for each case. Index 4 corresponds to the angular momentum compensation condition.

Index	1	2	3	4	5	6	7
M_{TM} (kA/m)	910	900	890	880	870	860	850
M_{RE} (kA/m)	860	840	820	800	780	760	740
δ_s (10^{-7} J·s/m^3)	–1.86	–1.24	–0.62	0	0.62	1.24	1.86

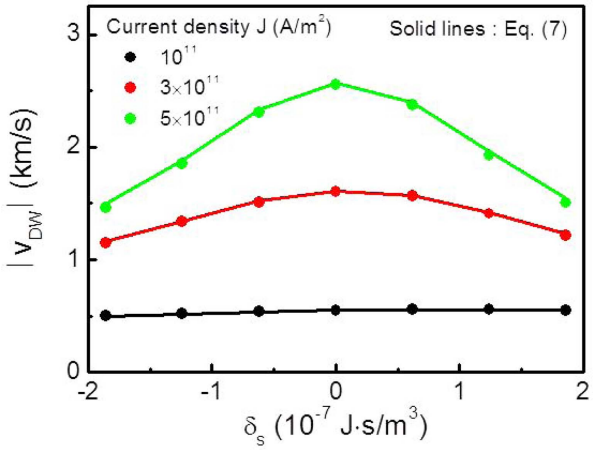

Fig. 1. (Color online) The domain wall velocity $|v_{DW}|$ as a function of the net spin density δ_s. Symbols are the numerical results, and the solid lines represent Eq. (7). The DMI constant is D_{sim} = 0.05 meV.

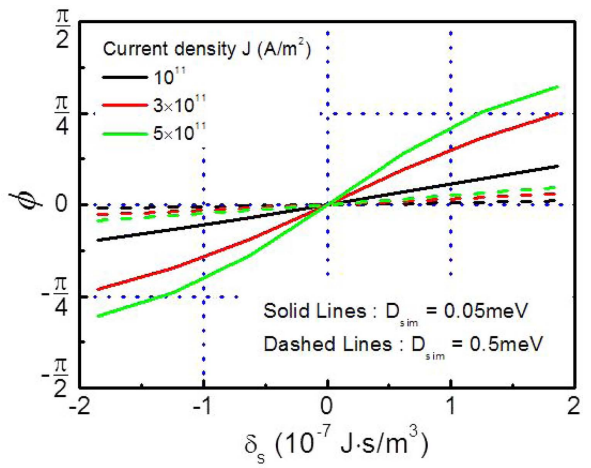

Fig. 2. (Color online) The domain wall angle ϕ as a function of the net spin density δ_s. Solid lines are for the case of D_{sim} = 0.05 meV, and dashed lines are for the case of D_{sim} = 0.5 meV. All data are obtained from the numerical calculation.

sets the initial angle as $\phi = 0$ for these calculations. There is no domain wall angle tilting at the angular momentum compensation point (i.e., $|\delta_s| = 0$). For nonzero $|\delta_s|$, the domain wall angle tilting increases with $|\delta_s|$. For a positive (negative) δ_s, the domain wall angle ϕ tilts counter-clockwise (clockwise). The large DMI suppresses the angle tilting strongly. All these features shown in Figs. 1 and 2 are consistent with the conceptual explanation given above.

To summarize, we study the dynamics of ferrimagnetic domain wall driven by damping-like spin-orbit torque for arbitrary compensation conditions. The maximum of domain wall velocity appears at the angular momentum compensation condition ($\delta_s = 0$). This tendency is caused by the fact that $\dot{X}$ and $\dot{\phi}$ are completely decoupled at the angular momentum compensation point. In other words, the domain wall angle ϕ does not vary with the damping-like torque at this condition. Therefore, the domain wall velocity can increase linearly with the current for $\delta_s = 0$ as for the case of antiferromagnet in Ref. [37]. It is worthwhile to compare field-driven dynamics of ferrimagnetic domain wall to damping-like-torque-driven one. In Ref. [40], field-driven domain wall velocity at the angular momentum compensation condition can be maximized in the high-field regime as well. In this case, domain wall velocity increases linearly because of no Walker breakdown phenomenon, resulted from the decoupling between $\dot{X}$ and $\dot{\phi}$ at the angular momentum compensation condition. We derive an explicit analytic expression of domain wall velocity and verify its applicability by comparing to numerical results. We expect that the analytic expression will be useful for both fundamental physics and applications since it provides a way to estimate essential physical parameters from experimental results and to design practical domain wall devices employing ferrimagnets, especially when the compensation is an important variable.

Acknowledgment

We acknowledge S.-K. Kim for fruitful discussions. This work is supported by the National Research Foundation of Korea (NRF) (Grants No. 2015M3D1A1070465 and No. 2017R1A2B2006119) and the KIST Institutional Program (Project No. 2V05750).

References

[1] D. A. Allwood, G. Xiong, C. C. Faulkner, D. Atkinson, P. Petit, and R. P. Cowburn, Science **309**, 1688 (2005).
[2] S. S. P. Parkin, M. Hayashi, and L. Thomas, Science **320**, 190 (2008).
[3] N. L. Schryer and L. R. Walker, J. Appl. Phys. **45**, 5406 (1974).
[4] T. Ono, H. Mihajima, K. Shigeto, K. Mibu, N. Hosoito, and T. Shinjo, Science **284**, 468 (1999).
[5] D.-S. Han, S.-K. Kim, J.-Y. Lee, S. J. Hermsdoerfer, H. Schultheiss, B. Leven, and B. Hillebrands, Appl. Phys. Lett. **94**, 112502 (2009).
[6] M. Jamali, H. Yang, and K.-J. Lee, Appl. Phys. Lett. **96**, 242501 (2010).
[7] S.-M. Seo, H.-W. Lee, H. Kohno, and K.-J. Lee, Appl. Phys. Lett. **98**, 012514 (2011).
[8] P. Yan, X. S. Wang, and X. R. Wang, Phys. Rev. Lett. **107**, 177207 (2011).
[9] W. Jiang, P. Upadhyaya, Y. Fan, J. Zhao, M. Wang, L.-T. Chang, M. Lang, K. L. W.Wong, M. Lewis, Y.-T. Lin, J. Tang, S. Cherepov, X. Zhou, Y. Tserkovnyak, R. N. Schwartz, and K. L. Wang, Phys. Rev. Lett. **110**, 177202 (2013).
[10] S. Woo, T. Delaney, and G. S. D. Beach, Nat. Phys. **13**, 448 (2017).
[11] A. Yamaguchi, T. Ono, S. Nasu, K. Miyake, K. Mibu, and T. Shinjo, Phys. Rev. Lett. **92**, 077205 (2004).
[12] M. Yamanouchi, D. Chiba, F. Matsukura, and H. Ohno, Nature **428**, 539 (2004).
[13] M. Kläui, C. A. F. Vaz, J. A. C. Bland, W. Wernsdorfer, G. Faini, E. Cambril, L. J. Heyderman, F. Nolting, and U. Rüdiger, Phys. Rev. Lett. **94**, 106601 (2005).
[14] A. Thiaville, S. Rohart, É. Jué, V. Cros, and A. Fert, Europhys. Lett. **100**, 57002 (2012).
[15] S. Emori, U. Bauer, S.-M. Ahn, E. Martinez, and G. S. D. Beach, Nat. Mater. **12**, 611 (2013).
[16] K.-S. Ryu, L. Thomas, S.-H. Yang, and S. S. P. Parkin, Nat. Nanotechnol. **8**, 527 (2013).
[17] S.-W. Lee and K.-J. Lee, Proc. IEEE **104**, 1831 (2016).
[18] D. Ravelosona, D. Lacour, J. A. Katine, B. D. Terris, and C. Chappert, Phys. Rev. Lett. **95**, 117203 (2005).
[19] S.-W. Jung, W. Kim, T.-D. Lee, K.-J. Lee, and H.-W. Lee, Appl. Phys. Lett. **92**, 202508 (2008).
[20] I. M. Miron, K. Garello, G. Gaudin, P.-J. Zermatten, M. V. Costache, S. Auffret, S. Bandiera, B. Rodmacq, A. Schuhl, and P. Gambardella, Nature **476**, 189 (2011).
[21] L. Liu, C.-F. Pai, Y. Li, H. W. Tseng, D. C. Ralph, and R. A. Buhrman, Science **336**, 555 (2012).
[22] M. Cubukcu, O. Boulle, M. Drouard, K. Garello, C. O. Avci, I. M. Miron, J. Langer, B. Ocker, P. Gambardella, and G. Gaudin, Appl. Phys. Lett. **104**, 042406 (2014).
[23] H. Kurebayashi, J. Sinova, D. Fang, A. C. Irvine, T. D. Skinner, J. Wunderlich, V. Novák, R. P. Campion, B. L. Gallagher, E. K. Vehstedt, L. P. Zârbo, K. Výborný, A. J. Ferguson, and T. Jungwirth, Nat. Nanotechnol. **9**, 211 (2014).
[24] X. Fan, H. Celik, J. Wu, C. Ni, K.-J. Lee, V. O. Lorenz, and J. Q. Xiao, Nat. Commun. **5**, 3042 (2014).

[25] K. Garello, C. O. Avci, I. M. Miron, M. Baumgartner, A. Ghosh, S. Auffret, O. Boulle, G. Gaudin, and P. Gambardella, Appl. Phys. Lett. **105**, 212402 (2014).
[26] X. Qiu, K. Narayanapillai, Y. Wu, P. Deorani, D.-H. Yang, W.-S. Noh, J.-H. Park, K.-J. Lee, H.-W. Lee, and H. Yang, Nat. Nanotechnol. **10**, 333 (2015).
[27] C. Zhang, S. Fukami, H. Sato, F. Matsukura, and H. Ohno, Appl. Phys. Lett. **107**, 012401 (2015).
[28] R. Ramaswamy, X. Qiu, T. Dutta, S. D. Pollard, and H. Yang, Appl. Phys. Lett. **108**, 202406 (2016).
[29] P. M. Haney, H.-W. Lee, K.-J. Lee, A. Manchon, and M. D. Stiles, Phys. Rev. B **87**, 174411 (2013).
[30] Y.-W. Oh, S.-h. C. Baek, Y. M. Kim, H. Y. Lee, K.-D. Lee, C.-G. Yang, E.-S. Park, K.-S. Lee, K.-W. Kim, G. Go, J.-R. Jeong, B.-C. Min, H.-W. Lee, K.-J. Lee, and B.-G. Park, Nat. Nanotechnol. **11**, 878 (2016).
[31] V. P. Amin and M. D. Stiles, Phys. Rev. B **94**, 104419 (2016).
[32] V. P. Amin and M. D. Stiles, Phys. Rev. B **94**, 104420 (2016).
[33] K.-W. Kim, K.-J. Lee, J. Sinova, H.-W. Lee, and M. D. Stiles, Phys. Rev. B **96**, 104438 (2017).
[34] A. M. Humphries, T. Wang, E. R. J. Edwards, S. R. Allen, J. M. Shaw, H. T. Nembach, J. Q. Xiao, T. J. Silva, and X. Fan, Nat. Commun. **8**, 911 (2017).
[35] S.-h. C. Baek, V. P. Amin, Y.-W. Oh, G. Go, S.-J. Lee, G.-H. Lee, K.-J. Kim, M. D. Stiles, B.-G. Park, and K.-J. Lee, Nat. Mater. **17**, 509 (2018).
[36] V. P. Amin, J. Zemen, and M. D. Stiles, arXiv:1803.00593 (2018).
[37] T. Shiino, S.-H. Oh, P. M. Haney, S.-W. Lee, G. Go, B.-G. Park, and K.-J. Lee, Phys. Rev. Lett. **117**, 087203 (2016).
[38] S.-H. Yang, K.-S. Ryu, and S. S. P. Parkin, Nat. Nanotechnol. **10**, 221 (2015).
[39] R. A. Duine, K.-J. Lee, S. S. P. Parkin, and M. D. Stiles, Nat. Phys. **14**, 217 (2018).
[40] S.-H. Oh, S. K. Kim, D.-K. Lee, G. Go, K.-J. Kim, T. Ono, Y. Tserkovnyak, and K.-J. Lee, Phys. Rev. B **96**, 100407(R) (2017).
[41] K.-J. Kim, S. K. Kim, Y. Hirata, S.-H. Oh, T. Tono, D.-H. Kim, T. Okuno, W. S. Ham, S. Kim, G. Go, Y. Tserkovnyak, A. Tsukamoto, T. Moriyama, K.-J. Lee, and T. Ono, Nat. Mater. **16**, 1187 (2017).
[42] A. C. Swaving, and R. A. Duine, Phys. Rev. B **83**, 054428 (2011).
[43] K. M. D. Hals, Y. Tserkovnyak, and A. Brataas, Phys. Rev. Lett. **106**, 107206 (2011).
[44] E. G. Tveten, A. Qaiumzadeh, O. A. Tretiakov, and A. Brataas, Phys. Rev. Lett. **110**, 127208 (2013).
[45] S. K. Kim, K.-J. Lee, and Y. Tserkovnyak, Phys. Rev. B. **95**, 140404(R) (2017).
[46] L. D. Landau and E. M. Lifshitz, Electrodynamics of Continuous Media, Course of Theoretical Physics Vol. 8 (Pergamon, Oxford, 1960).
[47] J. Jensen and A. R. Mackintosh, Rare Earth Magnetism (Clarendon, Oxford, UK, 1991).